NIH Public Access
Author Manuscript
Ann Biomed Eng. Author manuscript; available in PMC 2014 February 01.

Published in final edited form as:
Ann Biomed Eng. 2013 February ; 41(2): 250–262. doi:10.1007/s10439-012-0658-5.

High content evaluation of shear dependent platelet function in a microfluidic flow assay

Ryan R. Hansen[1], **Adam R. Wufsus**[1], **Steven T. Barton**[1], **Abimbola A. Onasoga**[1], **Rebecca M. Johnson-Paben**[1], and **Keith B. Neeves**[1,2,*]

[1]Department of Chemical and Biological Engineering, Colorado School of Mines, Golden, CO 80401

[2]Department of Pediatrics, University of Colorado, Aurora, CO 80045

Abstract

The high blood volume requirements and low throughput of conventional flow assays for measuring platelet function are unsuitable for drug screening and clinical applications. In this study, we describe a microfluidic flow assay that uses 50 μL of whole blood to measure platelet function on ~300 micropatterned spots of collagen over a range of physiologic shear rates (50–920 s^{-1}). Patterning of collagen thin films (CTF) was achieved using a novel hydrated microcontact stamping method. CTF spots of 20, 50, and 100 μm were defined on glass substrates and consisted of a dense mat of nanoscale collagen fibers (3.74 ± 0.75 nm). We found that a spot size of greater than 20 μm was necessary to support platelet adhesion under flow, suggesting a threshold injury is necessary for stable platelet adhesion. Integrating 50 μm CTF microspots into a multishear microfluidic device yielded a high content assay from which we extracted platelet accumulation metrics (lag time, growth rate, total accumulation) on the spots using Hoffman modulation contrast microscopy. This method has potential broad application in identifying platelet function defects and screening, monitoring and dosing antiplatelet agents.

Keywords

platelet adhesion; platelet aggregation; flow assays; microfluidics; micropatterning

1. Introduction

Platelet adhesion and aggregation onto the subendothelial extracellular matrix play a critical role in the arrest of bleeding at the site of a vascular injury. The mechanisms of platelet adhesion and aggregation are shear stress dependent.[24] This dependency provides the motivation for developing flow-based *in vitro* methods of measuring platelet function. Flow-based devices for measuring platelet function include annular chambers, parallel-plate chambers, or cone-and-plate viscometers.[18] However, the high volume requirements (10–

*Corresponding author: kneeves@mines.edu, Tel: 01-303-327-3919, Fax: 01-303-273-3730.

Conflicts of interest None

Supporting Material Supplementary material includes figures of the μCP apparatus, image processing routine, immunofluorescent images of micropatterned CTF, and the layout and characterization of the msMFA. Supplementary Movies 1, 2, and 3 show platelet accumulation on 20, 50 and 100 μm CTF spots, respectively, using HMC microscopy. The colored circles represent the location of the CTF spots during whole blood flow assay. Supplementary Movie 4 shows the relative fluid velocity via fluorescence polystyrene beads in the six channels of the msMFA. Supplementary Movies 5, 6, and 7 show platelet accumulation in the msMFA on 50 μm CTP spots for donors 2, 3 and 4, respectively.

$watermark-text
$watermark-text
$watermark-text

$watermark-text

$watermark-text

$watermark-text

100 mL) and low throughput (one shear rate per experiment) of these devices make them unsuitable for drug screening and clinical applications.

Microfluidic devices have emerged as a suitable alternative to these conventional flow assays because of their decreased volume requirement.[22] A particularly desirable characteristic is the simultaneous analysis of platelet function over the range of physiologic shear stresses. Gutierrez et al. reported a multishear microfluidic device capable of spanning a 100–fold range of shear rates over surfaces coated with fibrinogen and type 1 collagen.[10] Commercial microfluidic systems are now available and have been used to study shear dependent platelet function.[6,21] Another advantage of microfluidic approaches is that channel geometries can be defined to mimic vascular features such as stenosed vessels and valves.[14,25,30]

The throughput of flow assays can be increased using micropatterning methods to define many focal “injury” sites within a single channel. For example, Okorie et al. used a microarray pin-tool to define hundreds of collagen or collagen-von Willebrand factor (VWF) spots within a parallel plate flow chamber.[19] The advantage of this pin-tool approach is that the composition of each spot can be different. The disadvantage is that the spot size is limited to greater than 150 μm, and therefore, may not be compatible with microfluidic channels that have dimensions on the order of 10–100 μm. Microfluidic patterning has been used to define 50–250 μm lines of collagen and VWF across the entire width of microfluidic channels in platelet adhesion and rolling assays.[15,17] However, the propensity for platelets to accumulate in the corners of channels on collagen lines can confound the data analysis.[17] An alternative approach that has not been used in platelet flow assays is microcontact printing (μCP) where `stamps' (typically elastomers) are used to transfer `ink' (proteins, lipids) to a surface. One challenge for using μCP for platelet adhesion flow assays is that the most common adhesive substrate, native collagen fibrils, has fiber lengths (1–100 μm) that may be larger than the desired feature size. An alternative adhesive substrate is reconstituted collagen thin films (CTF), which is a hydrogel like material polymerized from acid-solubilized collagen monomers.[11] However, there are few reports that we are aware of that use μCP to transfer either large fibrous proteins or hydrogels.

The objective of this study was to develop and validate an assay for high content evaluation of shear dependent platelet function. We use the term high content to refer to a growing class of cell-based screening methods that rely on well-plate or microfluidic formats in combination with microscopy modalities to measure cell phenotypes.[4,5] The added complication with platelet function is that it must be evaluated under flow. Our approach was to pattern CTF using μCP in combination with a multishear microfluidic flow assay (msMFA). Previously, we characterized CTF as an adhesive substrate for evaluating platelet adhesion, and one of our objectives was to determine the minimum CTF feature size that could support platelet adhesion.[11] We found that CTF spots defined by μCP need to be greater than 20 μm to support platelet adhesion at a wall shear rate 300 s^{-1}. By integrating arrays of 50 μm CTF spots into msMFA, we were able to measure platelet accumulation kinetics on ~300 spots over a range of shear rates that span the physiological range.

2. Materials and Methods

2.1 Materials

Mouse anti-type I collagen mAb was purchased from AbCam (#ab90395, Cambridge, MA). Alexa Fluor 488 conjugated goat anti-mouse IgG was obtained from Invitrogen (Grand Island, NY). Pacific Blue anti-human CD41 was obtained from BD Pharminogen (San Jose, CA) and used to label platelets in whole blood. The thrombin inhibitor Phe-Pro-Arg-chloromethylketone (PPACK) was purchased from Haematologic Technologies, Inc (Essex

$watermark-text

$watermark-text

$watermark-text

Junction, VT). Equine tendon type I collagen (fibrillar collagen) was purchased from Chrono-Log (Havertown, PA). Acid-solubilized bovine type I collagen (#C4243), bovine serum albumin (BSA) and all other chemicals were purchased from Sigma-Aldrich (St. Louis, MO). Phosphate buffer saline (PBS, pH 7.4), BSA buffer (1mg/mL BSA in PBS), and HEPES buffered saline (HBS, pH 7.2) were made in-house.

2.2 Microcontact stamping of collagen thin films (CTF)

Glass slides (75 mm × 25 mm) were functionalized with octadecyltrichlorosilane (OTS) according to previous protocols.[11] Microcontact stamps with a height of 10 μm were fabricated in PDMS using conventional soft lithography methods. Stamps consisted of an array of spots with diameters of 20, 50, or 100 μm with edge-to-edge spacing of 100 μm. Stamps were molded into a 10:1 base:catalyst ratio and were cleaned using 1 M HCl, followed by 5 min. sonication in acetone, 5 min. sonication in ethanol, and then dried with an air brush. Stamps were dried in a convection oven at 80°C for 20 min. to remove any residual organic solvents before being treated with a 30 W oxygen plasma for 30 sec. Immediately following plasma treatment, stamps were incubated with 100 μL of 100 μg/mL solutions of type I collagen in PBS for 15 min or 100 μg/mL fibrillar collagen in 5% glucose. Prior to PDMS incubation, type I acid solubilized collagen solutions were neutralized using 0.1 M NaOH for 1 hour to allow for fiber reconstitution. After incubation, stamps were gently rinsed with reverse osmosis (RO) filtered water (18 MO) to remove excess collagen fibers. Stamps were then contacted with the OTS-treated glass slides immersed in PBS buffer for 2 min. using a manual drill press stand (Dremel Rotary Tool Workstation, Model 220). Slides were placed on polyurethane foam backing (Rogers Corporation, # SF060) to minimize PDMS stamp deformation due to non-uniform or over-pressurized stamping (Suppl. Fig. 1). Printed substrates were gently rinsed with PBS, and then with RO water before being quickly dried with an airbrush. Collagen functionalized substrates were stored at 4°C and used within 7 days.

2.3 Characterization of micropatterned collagen substrates

Micropatterned CTF were labeled by immunofluorescence. Slides were blocked in 1 mg/mL BSA buffer for 1 hr., incubated with 2 μg/mL of a primary antibody (mouse anti-type I collagen) in 1 mg/mL BSA buffer for 90 min, then incubated with 40 μg/mL of a fluorescently labeled secondary antibody in 1mg/mL BSA buffer for 1 hr., and finally rinsed in 1× PBS and RO water and dried. Slides were cover-slipped with a 70% glycerol solution in water and imaged by confocal microscopy (FV10i, Olympus). Olympus Fluoview software (version 3.0a) was used to measure the integrated fluorescence intensity of each spot. Data was reported as the integrated fluorescence of a spot divided by the spot area in relative fluorescent units (RFU) per micron squared. Five separate areas within a stamp were measured to determine intra-stamp spot variability. Average fluorescence intensities from three separate stamps of each size were also measured to determine stamp-to-stamp variation. Atomic force microscopy (Nanoscope III, Veeco) was used to image the morphology of micropatterned CTF. Silicon cantilevers with reflective Al coating and a resonance frequency of 320 kHz and 42 N/m spring constant (TESPA probes, Veeco) were used in tapping mode. All images were captured at a scan rate between 1–2.5 Hz. Fiber thicknesses and surface roughness were analyzed with Veeco software and reported as the mean ± standard deviation of five images.

2.4 Whole Blood Collection and Preparation

Human blood was collected from healthy donors via venipuncture. Phlebotomy was conducted in accordance with the Declaration of Helsinki and under the University of Colorado, Boulder Institutional Review Board approval. Donors had not consumed alcohol within 48 hours prior to the draw, nor had they taken any prescription or over-the-counter

drugs within the previous 10 days. Whole blood was drawn into a syringe containing the thrombin inhibitor PPACK (75 μM). Pacific Blue anti-human CD41 was added to 1 mL of whole blood to a final concentration of 5 μg/mL and was incubated for 15 min. PPACK (1 μL of 5 mM) was added to 1 mL of whole blood every 30 min. after the draw. Whole blood was used within 1 hour of phlebotomy.

2.5 Investigation of platelet adhesion to different sized collagen spots

PDMS microfluidic devices were exactly the same as those used in Hansen et al.[11] Each device consisted of three independent channels (500 μm wide, 50 μm high, 10 mm long). Each channel was placed over an array of CTF spots with diameters of 20, 50, or 100 μm. The average wall shear rate within the channel was calculated by:

$$\bar{\gamma} = \frac{fRe \cdot Q}{2A^{1.5}} \quad (1)$$

$$fRe = \frac{12}{1 - \frac{192}{\pi^5}\varepsilon \tanh\left(\frac{\pi}{2\varepsilon}\right)(1+\varepsilon)\sqrt{\varepsilon}} \quad (2)$$

where $\bar{\gamma}$ is the average shear rate, Q is the volumetric flow rate, A is the channel cross sectional area, and ε is the channel aspect ratio (width (w) / height (h)). A wall shear rate of 300 s^{-1} was used for these spot size experiments. The wall shear rate profile across the width of the channel (x-direction) was calculated by:

$$\gamma_{wall}(x) = \frac{48Q}{\pi^2 h^2 w} \frac{\sum_{n=1,3,5,\ldots}^{\infty} \frac{1}{n^2}\left[1 - \frac{\cosh\left(n\pi\frac{x}{h}\right)}{\cosh\left(n\pi\frac{w}{2h}\right)}\right]}{\left[1 - \sum_{n=1,3,5,\ldots}^{\infty} \frac{192h}{n^5\pi^5 w}\tanh\left(n\pi\frac{w}{2h}\right)\right]} \quad \left(-\frac{w}{2} \le x \le \frac{w}{2}\right) \quad (3)$$

The shear rate profile was used to identify regions of non-constant shear rate (edge region) and regions of constant shear rate (analysis region). Eqs. 1–3 are valid for fully-developed, steady-state, unidirectional laminar (Re<2800) flow in a channel with a constant cross-sectional area.

Prior to use, all devices were cleaned with 1N HCl, followed by sonication with acetone and ethanol and incubation in a 5 mg/mL BSA solution for at least 45 min. to prevent nonspecific adsorption of plasma proteins. Micropatterned collagen substrates were also blocked in a 5 mg/mL BSA solution for 45 min. After thorough rinsing of the slides and devices in 1× PBS and RO water, the slides were dried and microfluidic devices were reversibly sealed to the slides by vacuum-assisted bonding[9]. A syringe pump (PHD 2000, Harvard Apparatus) and 500 μL glass syringes (1700 Gastight, Hamilton Co., Reno, NV) were used to pull blood through the channels for 5 min. at a wall shear rate of 300 s^{-1}.

2.6 Design and characterization of the multi-shear microfluidic flow assay

For the high content evaluation of shear dependent platelet function, the msMFA was designed to deliver six shear rates that span from 50 s^{-1} to 920 s^{-1}. Fig. 1 gives an overview of the design of the msMFA. The microfluidic devices used in the msMFA consist of four regions: (1) a single inlet that holds 60 μL of whole blood, (2) a binding region, containing six parallel channels that contact an array of micropatterned 50 μm collagen spots, (3) a set of resistor channels, and (4) a single outlet for tubing (Tygon®, 0.25 mm ID, 0.74 mm OD) that connects to a syringe. All channels have a height of 50 μm. The relative flow rate

$watermark-text $watermark-text $watermark-text

between the six channels is set by the length of the resistor channels. The overall resistance of each channel ($R_{channel,\,i}$) was calculated by:

$$R_{channel,i}=R_{binding,i}+R_{resistor,i} \quad (4)$$

$$R_i=\frac{3\mu L}{4wh^3}\left(1-\frac{192h}{\pi^5 w}\sum_{n=1,3,5,\ldots}^{\infty}\frac{\tanh\left(n\pi\frac{w}{2h}\right)}{n^5}\right)^{-1} \quad (5)$$

where *w*, *h*, and *L* are the channel resistors' width, height, and length, respectively. Channels in the binding region were designed to maintain a constant width (250 μm) and length (10 mm). The widths of the channels in the resistor region were either 250 μm (channel 6) or 100 μm (channels 1–5). The lengths of the resistor regions varied between 5 mm (channel 6) and 95 mm (channel 1) to yield a relative flow rate ratio of 1.75 between adjacent channels, which is below the critical ratio of 2.5 required to maintain a constant hematocrit between channels according to the Zweifach-Fung bifurcation law.[31]

The fluid velocity through the binding region of each channel was characterized by measuring the streaklines of fluorescently labeled beads. A suspension of 1 μm diameter fluorescent polystyrene microparticles PBS containing 1 mg/mL BSA was perfused through the device at a flow rate of 10 μL/min. The length of streak-lines in a single movie frame was calculated using ImageJ software and was divided by the exposure time to obtain average bead velocities. Thirty to forty beads were captured per frame and five independent frames were analyzed for each flow condition. Bead velocities were also measured during whole blood assays to determine whether the platelet accumulation on CTF spots affected the hydrodynamic resistance in individual channels or the relative resistance between channels.

2.8 Investigation of shear dependent platelet function in the msMFA

The preparation procedures of the microfluidic devices and micropatterned glass substrates for the msMFA were exactly the same as described in Section 2.5. All micropatterned substrates used in the msMFA contained collagen arrays of 50 μm spots. Devices were manually aligned with the micropatterned substrate such that the collagen array intersected the binding region of the device as shown in Fig. 1. Whole blood was perfused through the msMFA at 10 μL/min. There were 3 to 6 spots per channel during the flow assays, and 25 to 50 spots imaged in each channel after the assay. The number of spots per channel depended on how the channel was aligned with respect to the spot array.

2.8 Image analysis and statistics

Platelet accumulation during the flow assay was imaged by Hoffman modulation contrast (HMC)[12] (40X, NA 0.60 or 20X, NA 0.45) on an inverted microscopy (IX81, Olympus) equipped with a motorized stage (Proscan III, Prior Scientific) and 16-bit CCD camera (ORCA-R2, Hamamatsu) controlled by Slidebook software v. 6.0 (Intelligent Imaging Innovations, Inc.). During an assay the stage cycled between each channel in a device. After 5 min., platelets were fixed by perfusion of 2.5% gluteraldehyde through the channel for 5 min., followed by removal of the device from the substrate. The substrates were cover slipped in an anti-fade buffer solution (F4680, Sigma-Aldrich). The surface coverage of platelets on each spot was calculated using a customized MATLAB (Mathworks, Natick, MA) routine that used the Sobel edge-finding routine to identify platelets in grayscale images, then the inside of contiguous edges was used to define a binary image (Suppl. Fig. 2). The surface coverage was defined as the area of platelets divided by the area of a spot. The kinetics of platelet accumulation on spots were characterized by three metrics: (1) the

$watermark-text $watermark-text $watermark-text

$watermark-text

$watermark-text

$watermark-text

lag time to 5% surface coverage of a spot; (2) the time to 30% surface coverage (SC_{30}); and (3) the growth rate (μ), which was the slope of the line defined by platelet surface coverage between the lag time and 95% surface coverage (%/min). End point platelet accumulation levels on spots were imaged by laser confocal microscopy. Integrated fluorescence intensity values of the platelet aggregates formed on the CTF spots were measured using Olympus Flouview software and normalized by the spot area. All data is reported as the mean ± standard deviation, except platelet accumulation data between donors, which was reported as the mean ± standard deviation of the mean. Differences between shear rates for each metric (lag time, SC_{30}, μ, end point integrated fluorescence intensity) and differences between spots within a channel was determined by Kruskal-Wallis ANOVA followed by Tukey's honestly significant difference criteria to determine differences between pairs.

3. Results

3.1 Characterization of micropatterned collagen substrates

CTF adsorbed to hydrophilic PDMS stamps were transferred onto OTS-modified (hydrophobic) glass slides immersed in PBS. CTF spots appear uniform and reproducible across the OTS substrate for spot sizes of 20, 50, and 100 μm (Fig. 2). A comparable density of collagen was transferred at each spot size based on immunofluorescence (Table 1). The variation between spots within an individual stamp (CV_{stamp}), and across multiple stamps (CV_{exp}), is an important parameter in developing a reproducible assay. Each spot size shows similar inter-stamp variation (CV_{stamp} = 11–13%) and intra-stamp spot variation (CV_{exp} = 21–30%). The amount of the CTF transferred from the PDMS stamp to the OTS modified glass substrate was measured by immunofluorescence of collagen on the stamps before and after transfer. There was no greater than a 34% decrease in fluorescence intensity after stamping (n = 3), suggesting that not all of the CTS was transferred to the substrate.

An aqueous transfer media was necessary to achieve good pattern transfer of CTF. Stamping of dehydrated CTF in air onto OTS treated slides resulted in poorly defined spots that were often partially or completely detached from the surface (Suppl. Fig. 3). Furthermore, use of a hydrophobic substrate was important for promoting good pattern transfer. CTF stamping to untreated, clean glass slides in a hydrated environment also resulted in poorly defined spots and poor adhesion.

The nanoscale structure of the micropatterned CTF was measured by AFM. OTS regions outside collagen spots appeared smooth with a root mean squared surface roughness of $R_{RMS,\ glass}$ = 0.39 ± 0.03 nm. Images of collagen spots contained a dense film of entangled collagen fibers characteristic of a collagen gel with a corresponding increase in roughness, $R_{RMS,\ collagen}$ = 1.2 ± 0.16 nm (Fig. 3). The average diameter of collagen fibers was 3.74 ± 0.75 nm.

3.2 Measuring and isolating channel edge effects

Channels with rectangular geometries have a non-constant shear rate profile, with the shear rate approaching zero at the corners (Fig. 4A). Using the μCP approach, we can isolate those spots found in in the edge region where gradients in shear rate are high. We defined the edge region as the upper and lower 10% of each channel ($-250\ \mu m \le y_{edge} \le -200\ \mu m$, $200\ \mu m \le y_{edge} \le 250\ \mu m$), and the analysis region was defined as the middle 80% of the channel ($-200\ \mu m \le y_{analysis} \le 200\ \mu m$). The shear rate remains relatively constant (4% change from its maximum value) across the analysis zone. Platelets accumulate at higher levels and with more variation in the edge region compared to the analysis zone (Fig. 4B). For experiments on 100 μm spots, the integrated fluorescence on the spots within the edge region is I_{edge} = 4150 ± 2280 RFU/μm^2 (n = 20), while within the analysis region the integrated fluorescence

$watermark-text

$watermark-text

$watermark-text

is $I_{analysis}$ = 1330 ± 670 RFU/μm^2 (n = 25). Exclusion of edge spots in analysis of platelet accumulation improves the variation noted between replicate spots ($CV_{,overall}$=82% to $CV_{analysis}$= 50%). For all data presented in Sections 3.3 and 3.4, only spots that were 75% or more in the analysis region were analyzed and reported.

3.3 Investigation of platelet adhesion to different sized CTF spots

The effect of spot size (20, 50, and 100 μm) on platelet adhesion and aggregation was measured in whole blood flow assays performed at an average wall shear rate of 300 s^{-1} for 5 min. Platelet surface coverage was calculated from HMC images using a Sobel edge finding routine (Suppl. Fig. 2). HMC is a brightfield technique that accentuates phase gradients to yield a pseudo-relief image similar to those achieved by differential interference contrast (DIC) but with the advantage that the microscopy does not need to be performed on a coverslip.[12] We used HMC for kinetic measurements because we found that epifluorescence microscopy of platelets (Pacific Blue labeled anti-CD41 antibody) during a whole blood flow assays tends to underestimate platelet accumulation. Representative platelet accumulation kinetics on spots of each size is shown in Fig. 5 and videos of platelet aggregation to each spot size are shown in Suppl. Movies 1 (20 μm spot), 2 (50 μm spot), and 3 (100 μm spots). Since we were only able to extract two-dimensional data (surface coverage) from HMC, we used integrated fluorescence intensity as an indirect measure of platelet aggregate size (Table 2).

For kinetic measurements on 50 μm and 100 μm spots, we observed rolling and adhesion of individual platelets onto spots in the first 1–2 min. of the assay. This was followed by aggregation of platelets to the initially adhered platelets. Every 100 μm spot across all donors supported platelet adhesion and aggregation (Table 2). Adhesion to 50 μm spots varied between donors. In three of the six donors, all 50 μm spots had significant platelet accumulation. However, in the other three donors only 60–70% of the 50 μm spots supported platelet adhesion. The density of platelets was comparable on 50 μm and 100 μm spots as measured by fluorescence intensity (Table 2), so differences in adhesion between the two spots were likely attributed to their size. On 20 μm spots (n=570), platelets were unable to firmly adhere to CTF for any of the donors, despite the fact that these spots contain a similar collagen surface density as the larger spots (Table 1). Platelets occasionally roll over 20 μm spots as evidenced by the spikes in the transient platelet surface area data (Fig. 5B); however, they do not firmly adhere. These data suggest that a threshold spot size exists of greater than 20 μm for stable platelet adhesion to CTF.

3.4 Characterization of fluid velocity in the msMFA

The average velocity within each of the six channels of the msMFA was calculated based on measurements of streaklines of fluorescent polystyrene beads (Suppl. Fig. 4, Suppl. Mov. 4). From the average velocity a flow rate in each channel was calculated (Q = <v>A), and this channel flow rate was used to calculate the average wall shear rate (Eq. 3). At a total flow rate of 10 μL/min, the measured wall shear rates in the six channels were 50, 90, 170, 320, 470, and 920 s^{-1}. The flow rate ratio between adjacent channels was 1.77 ± 0.24, which fall below the critical flow rate ratio to maintain a constant hematocrit.[31] Each measured shear rate falls within experimental error of the theoretical shear rates as calculated by Eqs. 3–5 (Supp. Fig. 4).

3.5 Shear dependent platelet accumulation in the msMFA

Platelet accumulation was measured on 50 μm CTF spots in the msMFA. We chose an array of 50 μm spots because this size was deemed a good trade-off between throughput and the ability to support platelet adhesion (Section 3.2). This array provides ~50 separate spots in each of the six channels. The kinetics of platelet accumulation on CTF spots in the msMFA

$watermark-text

$watermark-text

$watermark-text

was monitored by HMC (Fig. 6A). Non-specific platelet adhesion in the binding or resistor regions was not observed in any of the experiments. In a separate experiment, we measured bead velocities during a whole blood flow assay in the msMFA over CTF spots. There was no observable change in the fluid velocity in any of the channels over a 5 min. assay and there was no change in the relative fluid velocity between channels. We conclude from these data that platelet accumulation on the CTF spots was not significantly affecting the hydrodynamic resistance within the device over the timescale of the experiment.

The lag time, time to 30% surface coverage (SC_{30}) and growth rate (μ) as defined in Section 2.8 were measured on three to six spots at each shear rate across four different donors. The lag time was insensitive to shear rate, with only 470 s^{-1} having a significant ($p = 0.04$) difference compared the other shear rates (Fig. 6B). The SC30 significantly ($p = 0.02$) decreased with increasing shear rate from 50 s^{-1} to 470 s^{-1}, followed by an increase at 920 s^{-1} (Fig. 6B). The trend in the growth rate was an increase with increasing shear rate. There was significantly ($p = 0.002$) faster growth at 470 s^{-1} and 920 s^{-1} compared to the lower four shear rates. Sudden drops in platelet surface coverage corresponded to the shedding of platelet aggregates from the CTF spot. This phenomenon was usually observed at the latter stages of aggregate growth (Suppl. Movie 5). For example, the dip in the platelet area at ~3.5 min. at a wall shear rate of 470 s^{-1} in Figure 6A.

The variability in platelet accumulation was quantified by measuring the integrated fluorescence intensity and calculating the coefficient of variation (CV) on each spot at each shear rate (Fig. 7, Table 3). The variability was fairly consistent between donors 1, 3 and 4. Donor 2 had a significantly lower CV than the other three donors. The overall variability was $CV_{ave} = 27\% \pm 14\%$, which represents the variation in integrated fluorescence intensity per unit area of replicate spots averaged across all six shear rates and all donors ($n = 4$). The CV in end-point fluorescence between replicate spots for a given shear rate varied between donors (CV range: 10–37%). There were no trends in CV as function of wall shear rate. Qualitatively, we observed that the perturbation in the flow field caused by an upstream spot could affect platelet accumulation on an adjacent downstream spot in one donor. Suppl. Movie 6 (donor 3) shows that the perturbation of the flow field by the aggregates can be visualized by the pseudo-streamlines formed by the flowing blood cells. However, there seems to be little perturbation of the flow field in the cases of more moderate platelet aggregation as shown in Suppl. Movie 7 (donor 4), which was representative of the other three donors. An increase in total platelet accumulation levels with increasing shear rate is noted up to a shear rate of 320 s^{-1}, followed by similar level of accumulation on shear rates of 300, 470 and 920 s^{-1} (Fig. 7B). There was not a statistically significant difference in end-point platelet accumulation from the upstream to the downstream edge of the CTF spot array across all donors (Fig 7C).

A side-by-side comparison was conducted between patterned fibrillar collagen and CTF. Both collagens were adsorbed to stamps at 100 μg/mL. Fibrillar collagen fibers transferred onto OTS modified glass, but did form sharp features like the CTF (Fig. 8A). Some of the fibrillar collagen fibers were apparently larger than the stamp feature (50 μm) and extended well beyond the edge of the stamps. Two msMFA assays were ran simultaneously with the same donor, one on fibrillar collagen and one on CTF. Platelets aggregates on fibrillar collagen were both more diffuse and less dense compared to CTF at every shear rate. Representative images at 170 s^{-1} are shown in Fig. 8B and 8C.

4. Discussion

This study was motivated by the need for methods to perform high content evaluation of shear dependent platelet function for diagnostic and drug screening applications. To that

$watermark-text

$watermark-text

$watermark-text

end, we developed a novel μCP method for patterning collagen thin films in an aqueous environment on glass slides with spot sizes of 20–100 μm. We observed that platelet adhesion was not supported by 20 μm spots at 300 s^{-1}. Platelet adhesion and aggregation were supported on 50 μm and 100 μm spots at 300 s^{-1}, and on 50 μm spots at 50–920 s^{-1}. Integration of micropatterned collagen into a multishear microfluidic device provided a means to measure kinetic platelet accumulation rates on a subset of spots as well as end-point platelet accumulation on ~50 individual test sites at each shear rate with 50 μL of whole blood.

Pepsin digested, acid solubilized and collagen peptides have been previously patterned by μCP.[8,23] However, the triple helix quaternary structure of polymerized collagen is a necessary feature of to support platelet adhesion and to induce activation by outside-in platelet signaling through the GPVI receptor.[7,11] Therefore, reconstituted or native collagen fibers that contain a triple helix must be used in platelet adhesion flow assays. Microcontact printing of native type 1 fibrillar collagen was unsuccessful because the fiber sizes were larger than the features we attempted to stamp. In addition, the density of the fibrillar collagen was apparently less than the density of fibers in CTF based on the small, diffuse platelet aggregates observed on fibrillar collagen. Consequently, CTF offer good alternative to native fibrillar collagens especially for microfluidic formats. The fibers of the CTF are not as potent of a platelet agonists as fibrillar collagen[11], but they can be patterned in repeatable and homogeneous manner at the micrometer length scale.

In a previous study, we found that CTF can bind VWF with high affinity and support platelet adhesion at arterial shear rates (1000 s^{-1}).[11] Here, we were able use μCP to define CTF spots down to 20 μm. This is the first report that we are aware of that has demonstrated μCP of reconstituted collagen hydrogels. The best pattern transfer of CTF was achieved between a hydrophilic PDMS stamp and a hydrophobic glass substrate. Typically μCP is performed in air with dehydrated proteins[2]; however, we found poor pattern transfer of dehydrated CTF under these conditions. This poor transfer is possibly due to shrinkage induced by drying the hydrogel-like CTF, and thus causing delamination from the stamp and poor contact with the glass substrate. However, using submerged μCP in an aqueous environment, similar to the approach described by Bessuellie et al.[3], we were able achieve good pattern transfer.

We have not directly measured whether all of receptor-ligand interactions known to be important in thrombus formation in vivo interact with CTF. These receptor-ligand pairs include GPIb-VWF, GPVI-collagen, $\alpha_2\beta_1$-collagen, and $\alpha_{2b}\beta_3$-fibrinogen[24]. Platelets adhesion at arterial shear rates and platelet aggregation at all shear rates observed in this study is indirect evidence that GPIb-VWF and $\alpha_{2b}\beta_3$-fibrinogen interactions occur on CTF, respectively. Previous reports using pepsin digested and reconstituted collagens show that platelet adhesion to these substrates is absolutely dependent on $\alpha_2\beta_1$, while both collagen receptors (GPVI and $\alpha_2\beta_1$) are important for adhesion to native fibrillar collagen[26,28]. The relative role of GPVI and $\alpha_2\beta_1$ on adhesion to CTF remains to be determined.

The fiber morphology of stamped CTF appears slightly different than that of previously reported CTF deposited onto hydrophobic substrates under analogous conditions.[11] Fibers polymerized in bulk solution for 60 min. and then adsorbed to PDMS stamps for 15 min. are thinner than those formed by grown directly OTS modified glass (3.4 ± 0.74 nm compared to 7.4 ± 1.1 nm diameter). The formation of thinner fibers on hydrophilic substrates compared to hydrophobic substrates has been previously reported.[9] The precise mechanism of how surface wettability affects collagen fiber assembly is unknown, but collagen has higher affinity and higher surface mobility on hydrophobic surfaces.

$watermark-text

$watermark-text

$watermark-text

A spot size of greater than 20 μm was necessary to support stable platelet adhesion at a wall shear rate of 300 s^{-1}. This observation is in contrast with static platelet adhesion assays, where 2 μm fibrinogen spots were capable of capturing single platelets from whole blood.[1] The concept of a threshold injury size in flow-based models has been previously reported in the context of coagulation. Shen et al. showed that at a wall shear rate of 40 s^{-1}, the size of a tissue factor (TF) spot must be greater than 400 μm to induce a burst of thrombin generation in normal pooled plasma.[29] Our group found a similar threshold response in fibrin formation under flow, where even at a very high flux of thrombin from a 250 μm patch, we did not observe fibrin fibers formation above a wall shear rate of 50 s^{-1}.[16] In both of these examples, the threshold response to injury size is a function of the relative rates of solute transport and reaction kinetics. The observation of a threshold CTF spot size necessary to support stable platelet adhesion under flow is likely a function of receptor-ligand bond kinetics and outside-in signaling. We can envisage at least three scenarios to explain this observation: (i) platelets, even at venous shear rates, require a finite length of rolling, presumably GPIb-VWF mediated, before forming stable adhesion; (ii) the time scale of outside-in signaling is greater than the rolling time on the patch; therefore, the integrin $\alpha_2\beta_1$ does not take its active conformation; or (iii) sufficient contact area (number of bonds) between the platelet and the collagen is not achieved prior to reaching the end of the patch to resist the shear forces of the flowing blood. Determining which of these, or other, mechanisms are responsible for this observation will be the subject of future study.

We were able to identify dynamic trends in platelet adhesion and aggregation at six shear rates between 50 s^{-1} and 920 s^{-1} on CTF spots in the msMFA. Platelet accumulation can be divided into two events—adhesion to collagen and platelet-platelet aggregation—that can be partially decoupled by the lag time, SC_{30} and growth rate parameter extracted from kinetic measurements. The lag time is a measure of the time taken for the initial adhesion events between platelet and collagen to occur. The lag time was insensitive to shear, with no statistical difference over the range of shear rates measured. The SC_{30} decreases and the growth rate increases with increasing shear rate from the range of 50 s^{-1} to 470 s^{-1}. These data imply that the rate limiting step of platelet accumulation at these shear rates is the flux of platelets to the collagen surface. The growth rate is similar at 470 s^{-1} and 920 s^{-1} suggesting that platelet accumulation in this range no longer limited by platelet flux.

A challenge in flow-based cell screening methods, such as the one presented in this study is the cross-talk between upstream and downstream spots. The events that could influence cross-talk between spots include the transport of platelet agonists (thrombin, ADP, thromboxane A2) from an upstream site to a downstream site, the activation of platelets as they flow by, but do not necessarily adhere to, a test site, and perturbation of the flow field. Perturbation of the flow field was qualitatively noted in one of the videos (Suppl. Movie 5). However, there was no measureable difference in platelet accumulation as a function of downstream position across all donors. A more rigorous methodology such as particle image velocimetry (PIV) is likely necessary to quantify the precise hydrodynamic interactions between adjacent spots. An increase in spacing between spots beyond a critical distance could also mitigate potential confounding inter-spot events. The drawback of increasing spacing is a decrease in the throughput in terms of number test sites per channel. The distance between spots is also limited by design constraints of PDMS μCP stamps, where large spaces between features can result in roof collapse.[13] Alternative micropatterning approaches such as microstencils techniques may be better suited for more sparse patterns.[20]

Channels with rectangular geometries have a non-constant shear rate profile, with the shear rate approaching zero at the corners. Platelets tend to accumulate in the corners, which can confound data interpretation. These effects can be partially mitigated using high aspect ratio (width:height) channels.[27] However, when the adhesive substrate (i.e., collagen) spans the

width of the channel, it is difficult to decouple how platelet aggregates forming in the corners affect the shear stress, and thus, platelet adhesion and aggregation in the rest of the channel. By defining the CTF spots to be smaller than the channel, we were able to isolate these edge effects from platelet adhesion in the middle of the channel.

5. Conclusions

We have developed and characterized the msMFA as a high-content method for measuring platelet function over the physiologic range of shear rates. The novelty of this approach is the ability to make large number of replicate measurements of platelet accumulation across a physiologic of shear rates in a single assay with 50 μL of whole blood. We have shown that μCP of CTF provides a reproducible substrate that supports platelet adhesion for spots sizes greater than 20 μm. Owing to the low blood volume requirements, this method has promise for application in screening, monitoring and dosing of antiplatelet agents, as well as clinical applications in identifying platelet function defects such as von Willebrand disease and gray platelet syndrome.

Supplementary Material

Refer to Web version on PubMed Central for supplementary material.

Acknowledgments

This work was supported by a Scientist Development Grant (K.B.N.) and a Postdoctoral Fellowship (R.R.H) from the American Heart Association, the National Heart, Lung, and Blood Institute (HL100333), the Colorado Office of Economic Development and International Trade, and the Boettcher Foundation's Webb-Waring Biomedical Research Award.

References

1. Basabe-Desmonts L, Ramstrom S, Meade G, O'neill S, Riaz A, Lee LP, Ricco AJ, Kenny D. Single-Step Separation of Platelets from Whole Blood Coupled with Digital Quantification by Interfacial Platelet Cytometry (iPC). Langmuir. 2010 100217074141040. doi:10.1021/la9039682.
2. Bernard A, Renault J, Michel B, Bosshard H, Delamarche E. Microcontact printing of proteins. Adv Mater. 2000; 12:1067–1070.
3. Bessueille F, Pla-Roca M, Mills CA, Martinez E, Samitier J, Errachid A. Submerged Microcontact Printing (SμCP): An Unconventional Printing Technique of Thiols Using High Aspect Ratio, Elastomeric Stamps. Langmuir. 2005; 21:12060–12063. [PubMed: 16342970]
4. Bickle M. The beautiful cell: high-content screening in drug discovery. Anal Bioanal Chem. 2010; 398:219–226. [PubMed: 20577725]
5. Cheong R, Paliwal S, Levchenko A. High-content screening in microfluidic devices. Expert Opin. Drug Discov. 2010; 5:715–720. [PubMed: 21852997]
6. Conant CG, Schwartz MA, Beecher JE, Rudoff RC, Ionescu-Zanetti C, Nevill JT. Well plate microfluidic system for investigation of dynamic platelet behavior under variable shear loads. Biotechnol Bioeng. 2011; 108:2978–2987. [PubMed: 21702026]
7. Farndale RW, Sixma JJ, Barnes MJ, de Groot PG. The role of collagen in thrombosis and hemostasis. J Thromb Haemost. 2004; 2:561–573. [PubMed: 15102010]
8. Fukuda J, Sakai Y, Nakazawa K. Novel hepatocyte culture system developed using microfabrication and collagen/polyethylene glycol microcontact printing. Biomaterials. 2006; 27:1061–1070. [PubMed: 16111746]
9. Gurdak E, Rouxhet PG, Dupont-Gillain CC. Factors and mechanisms determining the formation of fibrillar collagen structures in adsorbed phases. Colloid Surface B. 2006; 52:76–88.

$watermark-text
$watermark-text
$watermark-text

$watermark-text

$watermark-text

$watermark-text

10. Gutierrez E, Petrich BG, Shattil SJ, Ginsberg MH, Groisman A, Kasirer-Friede A. Microfluidic devices for studies of shear-dependent platelet adhesion. Lab Chip. 2008; 8:1486–1495. [PubMed: 18818803]
11. Hansen RR, Tipnis AA, White-Adams TC, Di Paola JA, Neeves KB. Characterization of Collagen Thin Films for von Willebrand Factor Binding and Platelet Adhesion. Langmuir. 2011; 27:13648–13658. [PubMed: 21967679]
12. Hoffman R, Gross L. Modulation Contrast Microscope. Appl. Opt. 1975; 14:1169–1176. [PubMed: 20154791]
13. Hui C, Jagota A, Lin Y, Kramer E. Constraints on microcontact printing imposed by stamp deformation. Langmuir. 2002; 18:1394–1407.
14. Li M, Ku DN, Forest CR. Microfluidic system for simultaneous optical measurement of platelet aggregation at multiple shear rates in whole blood. Lab Chip. 2012; 12:1355. [PubMed: 22358184]
15. Nalayanda DD, Kalukanimuttam M, Schmidtke DW. Micropatterned surfaces for controlling cell adhesion and rolling under flow. Biomed Microdevices. 2007; 9:207–214. [PubMed: 17160704]
16. Neeves KB, Illing DAR, Diamond SL. Thrombin flux and wall shear rate regulate fibrin fiber deposition state during polymerization under flow. Biophys J. 2010; 98:1344–1352. [PubMed: 20371335]
17. Neeves KB, Maloney SF, Fong KP, Schmaier AA, Kahn ML, Brass LF, Diamond SL. Microfluidic focal thrombosis model for measuring murine platelet deposition and stability: PAR4 signaling enhances shear-resistance of platelet aggregates. J Thromb Haemost. 2008; 6:2193–2201. [PubMed: 18983510]
18. Nemerson Y, Turitto V. The effect of flow on hemostasis and thrombosis. Thromb Haemost. 1991; 66:272–276. [PubMed: 1745996]
19. Okorie UM, Diamond SL. Matrix protein microarrays for spatially and compositionally controlled microspot thrombosis under laminar flow. Biophys J. 2006; 91:3474–3481. [PubMed: 16905604]
20. Orth R, Wu M, Holowka D, Craighead H, Baird B. Mast cell activation on patterned lipid bilayers of subcellular dimensions. Langmuir. 2003; 19:1599–1605.
21. Philipose S, Konya V, Sreckovic I, Marsche G, Lippe I, Peskar B, Heinemann A, Schuligoi R. The Prostaglandin E2 Receptor EP4 Is Expressed by Human Platelets and Potently Inhibits Platelet Aggregation and Thrombus Formation. Arterioscl Throm Vas. 2010; 30:2416.
22. Prabhakarpandian B, Shen M-C, Pant K, Kiani MF. Microfluidic devices for modeling cell-cell and particle-cell interactions in the microvasculature. Microvascular Research. 2011; 82:210–220. [PubMed: 21763328]
23. Rozkiewicz DI, Kraan Y, Werten MWT, de Wolf FA, Subramaniam V, Ravoo BJ, Reinhoudt DN. Covalent Microcontact Printing of Proteins for Cell Patterning. Chem. Eur. J. 2006; 12:6290–6297. [PubMed: 16741908]
24. Ruggeri ZM, Mendolicchio GL. Adhesion Mechanisms in Platelet Function. Circulation Research. 2007; 100:1673–1685. [PubMed: 17585075]
25. Runyon MK, Johnson-Kerner BL, Kastrup CJ, Van Ha TG, Ismagilov RF. Propagation of blood clotting in the complex biochemical network of hemostasis is described by a simple mechanism. J Am Chem Soc. 2007; 129:7014–7015. [PubMed: 17497790]
26. Sarratt KL, Chen H, Zutter MM, Santoro SA, Hammer DA, Kahn ML. GPVI and alpha2beta1 play independent critical roles during platelet adhesion and aggregate formation to collagen under flow. Blood. 2005; 106:1268–1277. [PubMed: 15886326]
27. Sarvepalli DP, Schmidtke DW, Nollert MU. Design Considerations for a Microfluidic Device to Quantify the Platelet Adhesion to Collagen at Physiological Shear Rates. Ann Biomed Eng. 2009; 37:1331–1341. [PubMed: 19440840]
28. Savage B, Ginsberg MH, Ruggeri ZM. Influence of fibrillar collagen structure on the mechanisms of platelet thrombus formation under flow. Blood. 1999; 94:2704–2715. [PubMed: 10515874]
29. Shen F, Kastrup CJ, Liu Y, Ismagilov RF. Threshold Response of Initiation of Blood Coagulation by Tissue Factor in Patterned Microfluidic Capillaries Is Controlled by Shear Rate. Arterioscl Throm Vas. 2008; 28:2035–2041.

30. Tovar-Lopez FJ, Rosengarten G, Westein E, Khoshmanesh K, Jackson SP, Mitchell A, Nesbitt WS. A microfluidics device to monitor platelet aggregation dynamics in response to strain rate micro-gradients in flowing blood. Lab Chip. 2010; 10:291. [PubMed: 20091000]

31. Yen RT, Fung YC. Effect of velocity of distribution on red cell distribution in capillary blood vessels. Am J Physiol. 1978; 235:H251–7. [PubMed: 686194]

$watermark-text

$watermark-text

$watermark-text

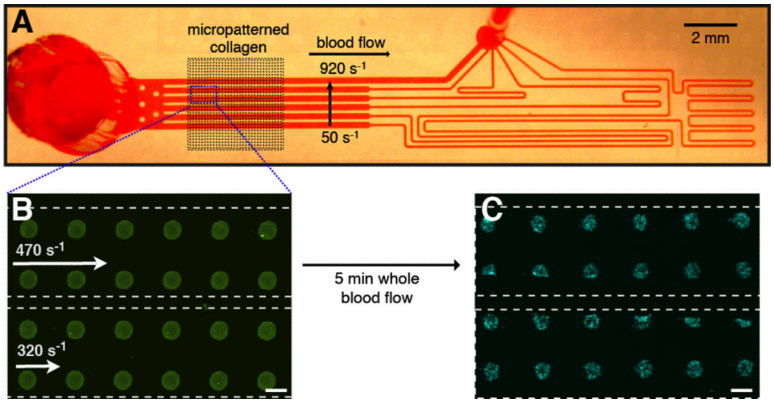

Figure 1.

Multishear microfluidic flow assay (msMFA) for high-content evaluation of shear dependent platelet function. (A) The msMFA is a six channel device reversibly bonded to a glass slide containing micropatterned CTF. The average wall shear rate in the channels from bottom to top is 50, 90, 170, 320 470, and 920 s^{-1}. (B) Immunofluorescence of 50 μm CTF spots within two of the msMFA channels. The dotted white line indicates the position of the walls of the channel. Scale bar = 50 μm. (C) Platelet aggregates on spots following a 5 min. flow assay of thrombin inhibited whole blood. Platelets are labeled with an anti-CD41 antibody (blue). Scale bar = 50 μm.

$watermark-text
$watermark-text
$watermark-text

$watermark-text

$watermark-text

$watermark-text

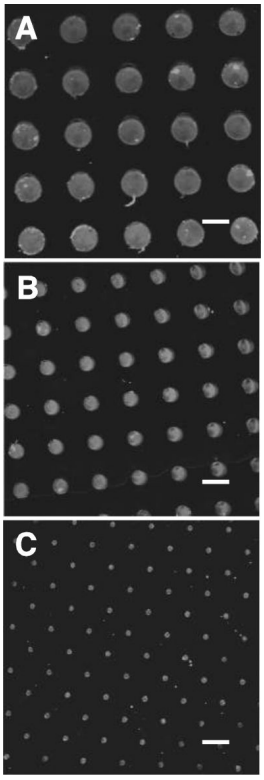

Figure 2.
Immunofluorescent images of micropatterned CTF on OTS glass substrates using stamps with (A) 100 μm spots, (B) 50 μm spots, and (C) 20 μm spots. Scale bar = 100 μm.

$watermark-text

$watermark-text

$watermark-text

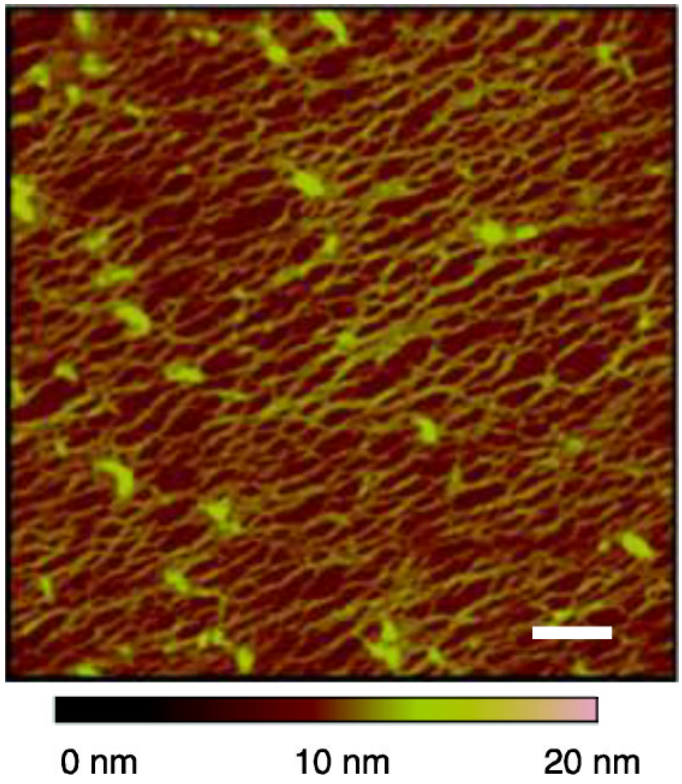

Figure 3.
AFM image of micropatterned CTF on OTS modified glass. Scale bar = 200 nm

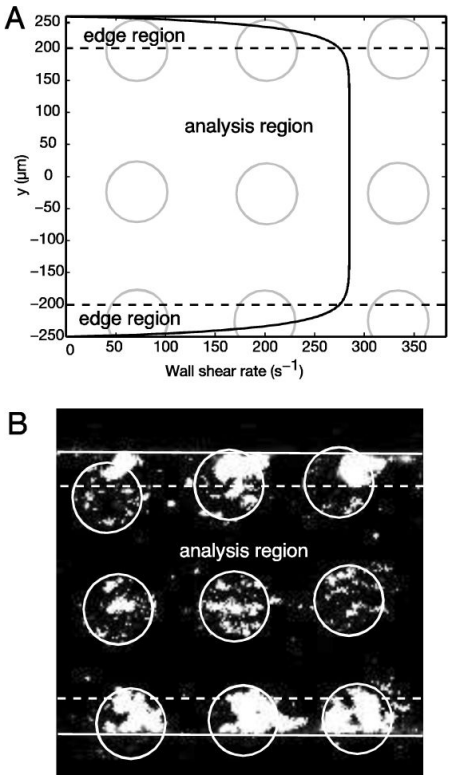

Figure 4.
Channel edge effects on platelet accumulation on CTF spots. (A) Shear rate profile across a microfluidic channel containing 100 μm spots and channel dimensions of w = 500 μm, h = 50 μm for a volumetric flow rate of 3.75 μL/min. Spots (gray circles) in the edge region (black dotted line) where there were sharp gradients in the shear rate profile were excluded from data analysis. (B) Fluorescent images of platelet aggregates on spots in the edge region and analysis zone after perfusion of thrombin-inhibited whole blood for 5 min. over 100 μm spots at a wall shear rate of 300 s^{-1}. White circles are the locations of the collagen spots, dotted white lines denote the edge region, and the solid white lines are the edges of the channel.

$watermark-text
$watermark-text
$watermark-text

$watermark-text
$watermark-text
$watermark-text

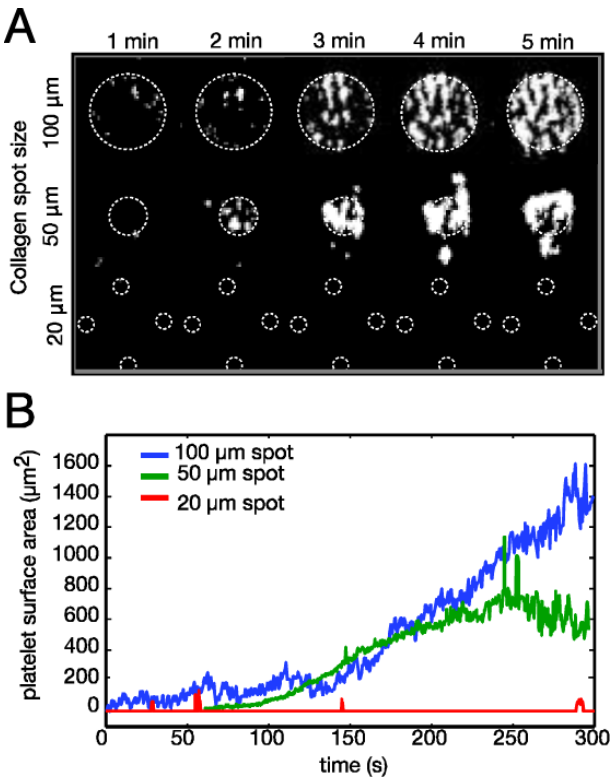

Figure 5.

Platelet accumulation kinetics over 20, 50 and 100 μm CTF spots. (A) Binary images of platelet aggregates on different sized spots during a 5 min. whole blood flow assay at a 300 s^{-1}. White dotted lines show the location of the CTF spot(s). (B) Surface area covered by platelets as a function of time and spot size. Platelet aggregates formed outside of the spot boundary are included in the analysis.

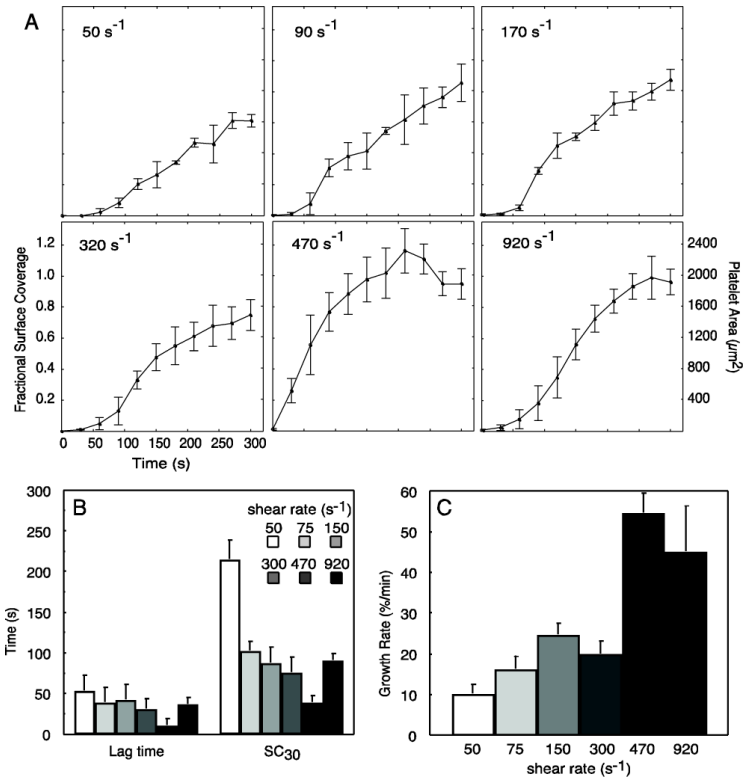

Figure 6.

Kinetic analysis of platelet accumulation on 50 μm micropatterned collagen spots. (A) Representative fractional surface coverage and surface area of platelet accumulation for each shear rate obtained during 5 min. perfusion of PPACK-inhibited whole blood from a single donor. Data is represented at mean ± standard deviation of 3 – 6 spots within a field of view. (B) Lag time (time to 5% platelet surface coverage) and time to 30% surface coverage (SC_{30}) obtained for each shear rate (n = 4 donors). (C) Kinetic growth rate constants obtained from spots during the growth phase (time between surface coverage greater than 5% and less than 90% of final surface coverage) at each shear rate (n = 4 donors). Data in parts (B) and (C) are represented at mean ± standard error of the mean between donors.

$watermark-text
$watermark-text
$watermark-text

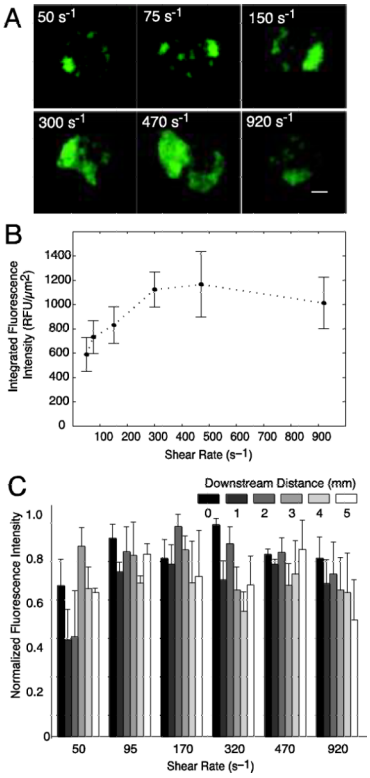

Figure 7.

End point analysis of platelet aggregates on 50 μm CTF spots after 5 min perfusions of whole blood through the msMFA. (A) Representative epifluorescence images of platelet aggregates formed over collagen at each shear rate measured. Scale bar = 10 μm. (B) End point integrated fluorescence intensity of platelet aggregates at each shear rate. (C) Normalized fluorescence intensity as a function of downstream distance for each shear rate. A downstream distance of 0 mm refers to the first spot that the flowing blood encounters. Fluorescence intensity was normalized by the maximum intensity for each donor in each channel. Data is the mean of four donors ± SEM.

$watermark-text
$watermark-text
$watermark-text

$watermark-text

$watermark-text

$watermark-text

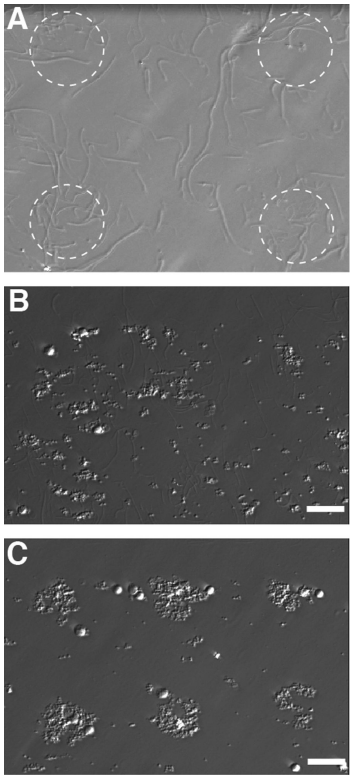

Figure 8.
Microcontact printing of fibrillar collagen. (A) Type 1 fibrillar collagen was transferred from stamps with 50 μm features (denoted by white dotted line) to OTS modified glass. Unlike CTF, patterning of fibrillar collagen did not result in sharp features. Representative images of platelet aggregates formed on patterned fibrillar collagen (B) and CTF (C) at 170 s^{-1} in the msMFA. Aggregates were smaller and more diffuse on fibrillar collagen compared to CTF. Scale bar = 50 μm.

$watermark-text

$watermark-text

$watermark-text

Table 1

Characterization of CTF spots. Collagen fiber density was measured by the integrated fluorescence from immunofluorescent labeled CTF spots. The coefficient of variation in integrated fluorescence intensity was measured within a stamp and between stamps.

Spot Size (μm)	Integrated fluorescence intensity (RFU/μm^2)	CV_{exp} [a]	CV_{stamp} [b]
20	980 ± 290	30%	13 ± 3%
50	1270 ± 270	21%	16 ± 2%
100	1030 ± 260	25%	11 ± 2%

[a] Coefficient of variation of average fluorescence intensity values from different stamps (n=3–4 stamps)

[b] Coefficient of variation of fluorescence intensity between spots within a single collagen stamp (n > 50 spots)

$watermark-text

$watermark-text

$watermark-text

Table 2

Platelet accumulation onto CTF spots after a 5 min. whole blood flow assay at 300 s^{-1}.

Spot Size (μm)	Integrated Fluorescence Intensity (RFU/μm²)[a]	% Spots aggregated[b]	Number of spot measured
20	590 ± 30	14 ± 2	570
50	3330 ± 1150	76 ± 14	530
100	2540 ± 770	100 ± 0	200
background	600 ± 30	N/A	1000

[a] averaged fluorescence intensities across 6 separate donors ± S.E.M.

[b] percentage of spots with mean integrated fluorescence intensity less than the local background plus one background standard deviation.

$watermark-text

$watermark-text

$watermark-text

Table 3

End-point platelet accumulation measured by confocal fluorescence microsopy on 50 μm CTF in the msMFA.

Donor	Average wall shear rate (s^{-1})	Integrated Fluorescence Intensity (RFU/μm^2)[a]	$CV_{channel}$[b]	CV_{device}[c]
1	50	700 ± 170	0.25	0.29 ± 0.13
	75	880 ± 380	0.43	
	150	1020 ± 340	0.33	
	300	2470 ± 430	0.17	
	470	2260 ± 300	0.13	
	920	2750 ± 1230	0.45	
2	50	1880 ± 360	0.19	0.13 ± 0.04
	75	2500 ± 341	0.17	
	150	2220 ± 230	0.11	
	300	2130 ± 210	0.10	
	470	2040 ± 210	0.10	
	920	1961 ± 240	0.12	
3	50	1180 ± 280	0.24	0.31 ± 0.12
	75	2020 ± 760	0.37	
	150	2590 ± 1180	0.46	
	300	3820 ± 870	0.23	
	470	5030 ± 780	0.16	
	920	3980 ± 1570	0.39	
4	50	2300 ± 750	0.33	0.36 ± 0.16
	75	2120 ± 760	0.36	
	150	2710 ± 650	0.24	
	300	3120 ± 690	0.22	
	470	2650 ± 950	0.36	
	920	1710 ± 1150	0.67	

[a] mean across 40–50 spots ± standard deviation

[b] coefficient of variation between spots in a channel

[c] mean coefficient of variation in a device ± standard deviation